Available online at www.sciencedirect.com
ScienceDirect
Mathematical Biosciences 208 (2007) 205–215
Mathematical Biosciences
www.elsevier.com/locate/mbs

Continuum description of a contact infection spread in a SIR model

Eugene B. Postnikov [a], Igor M. Sokolov [b,*]

[a] *Department of Theoretical Physics, Kursk State University, 305000, Radishcheva 33, Kursk, Russia*
[b] *Institut für Physik, Humboldt-Universität zu Berlin, Newtonstr. 15, D-12489 Berlin, Germany*

Received 4 January 2006; received in revised form 30 May 2006; accepted 2 October 2006
Available online 19 October 2006

Abstract

We consider the process of an epidemic spread in a population of individuals with low mobility within the SIR scheme. In a continuum limit such propagation mechanism is described by a non-linear reaction–diffusion equation with a diffusion coefficient being the function of the densities of susceptible. The traveling wave solution of the corresponding system of partial differential equations is obtained and analyzed. We show that the model allows for description of Kendall epidemic waves, and give the dependence of the infection wave's shape on the parameters of the system. An explicit calculation is done for realistic values of parameters obtained from field epidemiological data for a phocine distemper virus infection among harbor seals in 1988.

Keywords: Epidemic waves; SIR model; Diffusion; PDE

1. Introduction

Despite of a century of thorough work, the problem of mathematical description of spread of an epidemic is still an actual question, see for example the review [1], the book [2] and references

* Corresponding author. Tel.: +49 30 2093 7616; fax: +49 30 2093 7636.
E-mail address: igor.sokolov@physik.hu-berlin.de (I.M. Sokolov).

0025-5564/$ - see front matter
doi:10.1016/j.mbs.2006.10.004

therein. The standard SIR (Kermack–McKendrick) model [3] considers a system as consisting of three kinds of individuals which are the susceptible (S), the infected (I), and the removed (R) ones. It is assumed that a removed (i.e., recovered and immune or dead) individual can be never infected again. In the case of perfect mixing, the dynamics of population is described by a system of ordinary differential equations

$$\begin{aligned}\frac{\mathrm{d}S}{\mathrm{d}t} &= -kSI,\\ \frac{\mathrm{d}I}{\mathrm{d}t} &= kSI - \frac{1}{\tau}I,\\ \frac{\mathrm{d}R}{\mathrm{d}t} &= \frac{1}{\tau}I,\end{aligned} \tag{1}$$

where k is the rate of the infection transmission and τ is the characteristic recovery (or removal) time. If the birth or the introduction of new individuals into the system can be neglected on the timescales of the infection, the conservation law $S + I + R = C = \text{const}$ holds, and the system can be reduced to two equations. Here, $S(t)$, $I(t)$ and $R(t)$ are the numbers of susceptible, infected, and removed (recovered) individuals as functions of time, respectively.

It must be pointed out that the system above, corresponding to a mean-field approach fully neglecting any spatial structure of disease spreading, describes the population with the perfect mixing. Such an approach is definitely inapplicable for low population densities of slowly moving individuals. The standard method of including the spatial effects consists in the introduction of a of diffusion term, as discussed, e.g., by Murray [2]. For example, the equation for the distribution of infected and recovered individuals takes a form

$$\begin{aligned}\frac{\partial S}{\partial t} &= D\nabla^2 S - kSI,\\ \frac{\partial I}{\partial t} &= D\nabla^2 I + kSI - \frac{1}{\tau}I,\\ \frac{\partial R}{\partial t} &= D\nabla^2 R + \frac{1}{\tau}I.\end{aligned} \tag{2}$$

Now $S(\mathbf{x}, t)$, $I(\mathbf{x}, t)$, and $R(\mathbf{x}, t)$ are the densities of susceptible, infected, and removed (recovered) individuals, respectively, and the conservation law reads $S + I + R = C = \text{const}$, where C is the initial population density. Using this conservation law one can again reduce the system to a one of two equations,

$$\begin{aligned}\frac{\partial I}{\partial t} &= D\nabla^2 I + k(C - I - R)I - \frac{1}{\tau}I,\\ \frac{\partial R}{\partial t} &= D\nabla^2 R + \frac{1}{\tau}I.\end{aligned} \tag{3}$$

Under the values of parameters corresponding to the infection propagation, this system of equations shows solutions in form of traveling waves. Ref. [2] discusses its application to the spread of the Black Death. The discussion of this application shows however a drawback of the model: the population of the medieval Europe was not really mobile, so that even the susceptible individuals (let alone infected or dead ones) hardly performed unconfined diffusion [4]. Moreover, a

symmetric form of the infection wave represented by solutions of Eq. (3) does not resemble the forms of realistic infection waves, as they are depicted, e.g., in the *Atlas of disease distributions...* [5]. These waves (called Kendall waves in this Reference, after one of the pioneers of mathematical description of infection spread) have a steep front indicating initially fast increase of the disease incidence at a given site, followed by a much slower decay.

From the point of view of the mechanism of infection propagation in a low-mobility population the diffusion term, borrowed from the theory of diffusion-controlled reactions, looks a bit an artificial addition. It is especially clear in the case of plant diseases – plants do not move, and also the spread of the infective agents (like fungi considered in Ref. [6]) is a slow and spatially localized process. Nevertheless the infection waves appear also in this situation. In what follows, we consider infection wave propagation in a population of immobile individuals, where a local infection spread mechanism (between individuals or parts of the population in close contact) is present. The goal of this paper is to consider a variant of system of partial differential equations based on the consideration of the nearest-neighbor mechanism of the infection transmission, to present its numerical solutions for some special situations and to discuss its relevance to description of realistic epidemics.

2. The continuum model

The aim of the present article is to discuss a deterministic model for infection spread in a population of immobile individuals (like in plants) or of individuals showing a high degree of site fidelity (like harbor seals, whose habits are described, e.g., in Ref. [8]) where the mixing within the population located in one site is strong while the infection transmission between sites takes place only via contacts between individuals performing rare relatively long trips between sites.

The mechanism of infection spreading between immobile individuals corresponds to what is known as a 'contact process' in statistical physics. Let us start from the system on a lattice (Fig. 1), where each cell of the lattice represents an individual, as in the model of Ref. [7] pertinent to plant diseases, and can be in an either of three states, S, I or R. Let a be the lattice spacing and let us normalize the concentrations in such a way that the overall initial concentration $C = 1$. We restrict ourselves now to a two-dimensional situation on a square lattice. In each given realization, the probability for a given S-cell to change its state per unit time depends on the number of its infected neighbors. Let us take a probability of the infection of a given cell by one of its neighbors per unit time to be given by a rate $\kappa/4$ (same for all orientations), provided the corresponding cell is susceptible, and its neighbor is infected. We consider now the ensemble of equivalent systems and associate S, I, and R (measured in units of C) with probabilities (mean values over realizations) for a given cell to be in either of its possible states in a given realization of a process. The probability for a cell (x, y) to be infected can only change in case it is susceptible and is proportional to the number of its infected neighbors. On the average, we get

$$\Delta I(x,y) = \frac{\kappa}{4} S(x,y)[I(x+a,y) + I(x-a,y) + I(x,y+a) + I(x,y-a)]\Delta t \tag{4}$$

for the change of the probability of being infected due to new infections. We note that here the probability to find an infected cell, say at place $(x + a, y)$, in vicinity of a susceptible cell at

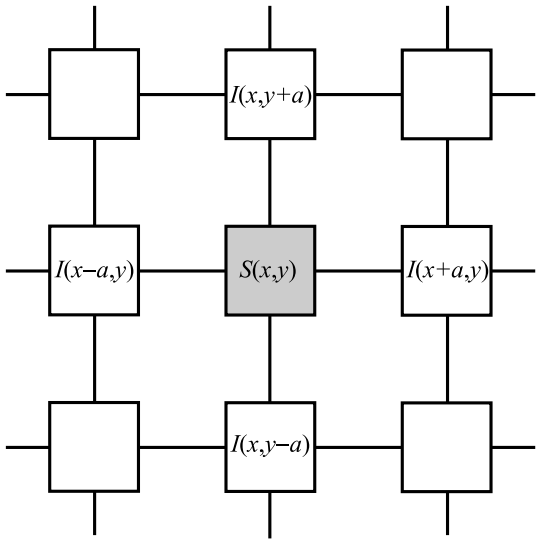

Fig. 1. Cell model for the infection of nearest neighbors.

(x, y) is taken to be the same as when the corresponding cell at (x, y) would be infected or removed, which puts our approach into the class of local mean field models (the class usual reaction–diffusion equations also belong to).

In a continuum limit, after expanding the terms in brackets up to the first non-vanishing term in a we get the partial differential equation

$$\frac{\partial I}{\partial t} = \kappa S\left(I + \frac{a^2}{4}\nabla^2 I\right), \tag{5}$$

which is a non-linear reaction-diffusion equation

$$\frac{\partial I}{\partial t} = \kappa SI + D(S)\nabla^2 I, \tag{6}$$

with the diffusion coefficient $D(S) = \tilde{D}S$ linear in the density of susceptible, with $\tilde{D} = \kappa a^2/4$ being the reaction-induced transport coefficient. This is a reasonable equation for immobile individuals since it describes the spread of infection into an non-infected population (effective diffusion of I) which stops if the susceptible population is absent. Moreover, it is definitely the simplest possible equation of this class (assuming the corresponding diffusion coefficient is simply proportional to the density of susceptible individuals) which could be simply postulated based on purely phenomenological 'Landau-like' considerations.

Another situation, to which the model is possibly applicable corresponds to populations of mobile individuals showing a high degree of site fidelity (like harbor seals, whose habits are described, e.g., in Ref. [8]) where mixing within the population located at one site is strong while the infection transmission between sites takes place only via contacts between individuals performing rare relatively long trips between neighboring sites. The argumentation for the case when a cell represents not a single individual but a typical well-mixed region of space is even simpler, since S, I, and R

can from the very beginning be considered as macroscopic variables pertinent to the cell. The overall system differs from Eq. (6) only by the existence of the additional term $\kappa_1 S(x, y)I(x, y)$ describing the rate of conversion $S \to I$ due to infection within a cell. The resulting equation is then the same Eq. (6) with the only change of the coefficient κ to $\kappa + \kappa_1$.

The infection front corresponding to this 'modified Fisher equation' was considered recently in [9]. We also note that our model is a special case of a general integral equation [10]. Our equation can be obtained from this one using the procedure analogous to the one used to obtain a Fokker–Planck equation from the integral Chapmen–Kolmogorov one, namely a kind of Kramers–Moyal expansion. We note that our equation is different from the one proposed in Ref. [11], since in their case the additional diffusion term has a form typically associated with the forward Kolmogorov equation (i.e., with concentration-dependent diffusion coefficient between the two differential operators, $\nabla D(S)\nabla I$), while in our case it has a 'backward' form, with diffusion coefficient in front of the differential operator.

Adding to Eq. (5) a recovery term, one gets:

$$\frac{\partial I}{\partial t} = \kappa(1 - R - I)I + \tilde{D}(1 - R - I)\nabla^2 I - \frac{1}{\tau} I, \qquad (7)$$
$$\frac{\mathrm{d}R}{\mathrm{d}t} = \frac{1}{\tau} I.$$

This system has three parameters controlling the spread process: a rate of infection transmission to the nearest neighbors κ, a transport coefficient $\tilde{D} = \kappa a^2/4$ (with a being the mean distance between the nearest-neighboring cells) and a mean recovery time τ. The last parameter can be exactly determined for a concrete disease, while κ and $\tilde{D}$ depend on the structure of the population through the typical mixing patch size and the mode of infection transmission between patches. We note that when S, I, and R are considered as probabilities, the dimension of κ is $[T^{-1}]$ and the one of $\tilde{D}$ is the one of the normal diffusion coefficient, $[\tilde{D}] = [L^2/T]$. Note that returning to 'normal' units will give us $k = \kappa C^2$, so that the propagation criterion for a modified Fisher wave obtained in what follows is the same as the one for the normal Fisher wave.

The note is in place that equations similar to Eq. (7) were already discussed in different, physical, contexts. Thus, the mechanism of effective diffusion emerging due to reactions was identified in fractal growth models in chemical catalysis [12]. A related approach was proposed by Ball et al. [13] for the continuum description of cluster growth in diffusion-limited aggregation (DLA) process. This first attempt was, however, not quite successful (it did not lead to a correct value of aggregate's fractal dimension). A modification of the approach done in a recent work, Ref. [14], taking into account the strong dependence of the effective reaction rate on the cluster's external perimeter, succeeded in giving a good approximation for this dimension.

3. The form of infection waves

Numerical solution of Eq. (7) for initial conditions in form of a concentrated peak suggest (for large enough recovery times) stable propagation of infection fronts. Let us concentrate on the one-dimensional situation, the one of a flat front (as reached also in 2d at later times). Let the front of a constant form propagate through the system at a constant velocity v. In a comoving

frame $x' = x - vt$ the form of the front given by $I(x')$, $R(x')$ is time-independent and governed by a system of two ordinary differential equations

$$\tilde{D}(1-R-I)\frac{\mathrm{d}^2}{\mathrm{d}x'^2}I + v\frac{\mathrm{d}}{\mathrm{d}x'}I + \kappa(1-R-I)I - \frac{1}{\tau}I = 0, \tag{8}$$
$$v\frac{\mathrm{d}}{\mathrm{d}x'}R + \frac{1}{\tau}I = 0.$$

Linearizing the first equation in the leading edge of the front ($I \to 0$, $R \to 0$) we get

$$\tilde{D}\frac{\mathrm{d}^2}{\mathrm{d}x'^2}I + v\frac{\mathrm{d}}{\mathrm{d}x'}I + \left(\kappa - \frac{1}{\tau}\right)I = 0.$$

The solution of this equation is a decaying exponential $I(x') \simeq \exp(-\lambda x')$, with λ fulfilling the equation

$$\tilde{D}\lambda^2 - v\lambda + \left(\kappa - \frac{1}{\tau}\right) = 0,$$

i.e.,

$$\lambda = \frac{v}{2\tilde{D}} \pm \sqrt{\left(\frac{v}{2\tilde{D}}\right)^2 - \frac{1}{\tilde{D}}\left(\kappa - \frac{1}{\tau}\right)}.$$

The fact that oscillating solutions are physically forbidden, gives us the minimal stable propagation velocity

$$v_{\min} = 2\sqrt{\tilde{D}(\kappa - \tau^{-1})}. \tag{9}$$

The propagation is possible if and only if $\kappa > \tau^{-1}$. The allowed front propagation velocities are $v \geqslant v_{\min}$; typical propagation velocities are close to $v_{\min}$ (marginal stability principle). This fact is corroborated by our numerical simulations.

Let us now turn to the rear front (tail) of the infection wave. Far behind the front, i.e., for $x' \to -\infty$ one has $I \to 0$ and $R \to R_- = \text{const}$ so that the linearization of both our equations gives

$$\tilde{D}(1-R_-)\frac{\mathrm{d}^2}{\mathrm{d}x'^2}I + v\frac{\mathrm{d}}{\mathrm{d}x'}I + \kappa(1-R_-)I - \frac{1}{\tau}I = 0,$$
$$v\frac{\mathrm{d}}{\mathrm{d}x'}R + \frac{1}{\tau}I = 0.$$

The solution of these equations are a growing exponential $I(x') \simeq A\exp(\gamma x')$ for I and a decaying function $R(x') \simeq R_0 - B\exp(\gamma_1 x')$ for R. From the second equation it follows immediately that $\gamma_1 = \gamma$. For realistic conditions, the continuous approximation is valid outside of the critical regime, i.e. when the patchiness of the pattern of removed following from the percolation approach [15,16] can be neglected, which corresponds to practically full conversion of susceptible into removed $R_- \to 1$. Substituting this into the first equation we get

$$\gamma = 1/v\tau > 0.$$

Let us estimate the values of the corresponding exponential increment factors at $v \approx v_{\min}$. For the front of the infection wave one has

$$\lambda \simeq \frac{2\sqrt{\tilde{D}(\kappa - \tau^{-1})}}{2\tilde{D}} = \frac{1}{\sqrt{\tilde{D}\tau}}\sqrt{\kappa\tau - 1}$$

while for its tail

$$\gamma \simeq \frac{1}{2\sqrt{\tilde{D}(\kappa - \tau^{-1})\tau}} = \frac{1}{2}\frac{1}{\sqrt{\tilde{D}\tau}}\frac{1}{\sqrt{k\tau - 1}}.$$

Thus, in strongly supercritical waves with $\kappa\tau > 3/2$, which correspond to a fast propagation into a non-infected region, one observes a steep front and a relatively flat tail, as observed for the Kendall waves in a fowl pest epizootic in England and Wales in 1970–1971 [5]. For weakly supercritical epidemics $k\tau \approx 3/2$ the front is approximately symmetric, and very close to criticality $\kappa\tau \approx 1$ (extinction) it assumes an inverse form with slow growth at a front and relatively faster decay in the tail. However, as stated above, the accuracy of the deterministic continuous approximation in this region is low, so that such regime might be absent in really observed epidemics.

4. Numerical results

In our numerical examples, we use realistic values of parameters obtained by comparison with the real dynamics of the epidemic of phocine distemper virus infection among harbor seals in 1988. This epidemic is a well-documented process, see the primary data collection in [17]. One of most successful theoretical description [8] uses the system of ordinary SEIR differential equations for the every group of seals. In our approach, we consider the spread of disease as a traveling wave process in the distributed population within a simpler SIR model. For the sake of simplicity, we use data sampled in relatively short region localized around (and in) Öresund from Anholt to Southwestern Baltic (see the map in [17]). It allows us to use one-dimensional form of equation since the epidemic have moved throw the thin strait in this region. Besides, various population in this region can be considered as continuum in consequence of large number of seals and relatively small distance between patches. The points of sampling are Anholt (0, 42, 46, 0), Hesselø (12, 60, 46, 40), Southern Halland (38, 73, 82, 70), Öresund (63, 103, 77, 110), and Southwestern Baltic (95, 120, 70, 142). The numbers in brackets mean consequently (the day from the beginning of epidemic when the first dead seal was detected, the day of 50% mortality, the percentage of dead seals of the initial patch's size, the approximate distance (km) from the source of epidemic). These data are based on [17] and geographical Atlas of this region. Corresponding points are represented at Fig. 2, where the points of the first record of disease marked with stars and the points of 50% mortality marked with circles. The slope of the dashed line drawn through the arithmetic mean of each pair of experimental points (dots) except the initial one allows us to determine the mean velocity of infection as approximately 1.43 km/day.

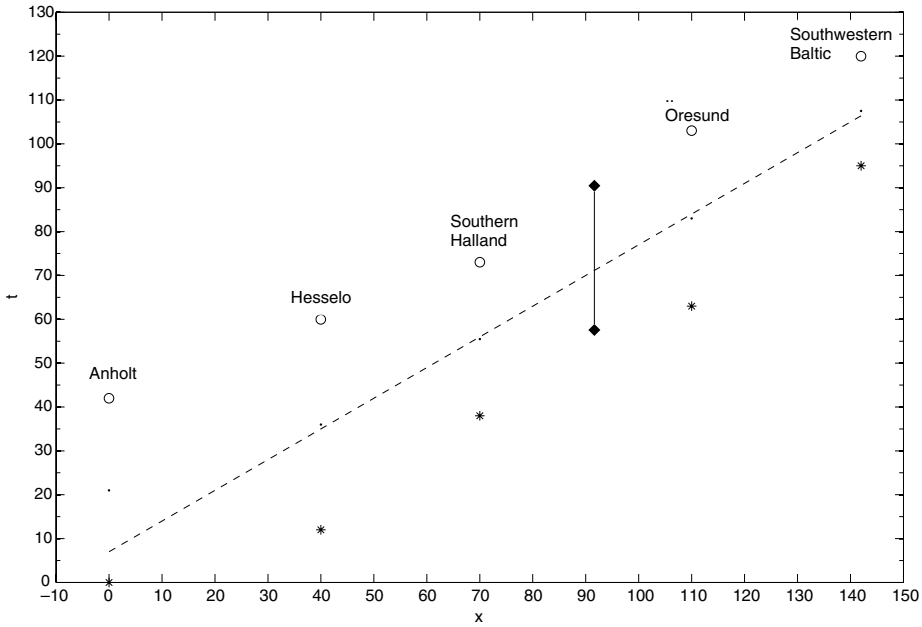

Fig. 2. Spatiotemporal dynamics of the epidemic among seals. The time of the first record of disease at a given site is marked with stars and the time 50% mortality with circles. The dashed line corresponds to the front propagation with the velocity obtained from the theoretical model. The width of the theoretical infection wave calculated as a time from the point where the theoretical number of infected is 1% of the maximal number to the point of 50% mortality is shown as a solid bar.

Following [8] and references therein the value $\tau = 15$ (days) is used. It is a value of the disease duration (note that authors of [8] use a more complicated SEIR model considering also infected but not-infectious individuals). As a mean radius of 'cells' we took $a = \sqrt{2}$ km. It is reasonable value for the strong mixing in the seal-rookery and useful for calculation: $a^2/2 = 1$, the denominator *2* corresponds to the linear geometry; $\kappa = 0.75$ is used as a probability to be infected. As an initial distribution of the infected seals a narrow 'half-Gaussian' with the dispersion a is used. We note that the values of parameters chosen reproduce well both the experimental infection wave velocity and width.

Equations are solved numerically using MATLAB. The spatial-time distribution of infected persons (epidemic wave's motion, Fig. 3b) for the first 50 days is represented at Fig. 3.

It can be pointed out that during about 10 days the initial distribution (Fig. 3e) is transformed to the stable infection wave spreading with the constant velocity $v_{\text{calc}} = 1.47$ km/day (Fig. 3b). This value shows a good agreement with the theoretical value $v_{\min} = 1.43$ km/day and confirms the marginal stability principle. The evolution of the front in 0, 5, 30, 50 days is shown in Fig. 3(e), (d), (c), and (a), respectively.

Fig. 4 represents the solution on the logarithmic scale (dashed line). The both forward and rear fronts of an infection wave can be fitted by straight lines over some interval. The slope of the backward tail is determined as 0.045 that is in the very good agreement with the theoretical value $\gamma = 0.047$. Calculated value of the forward front's slope is -0.76 vs. the theoretical value

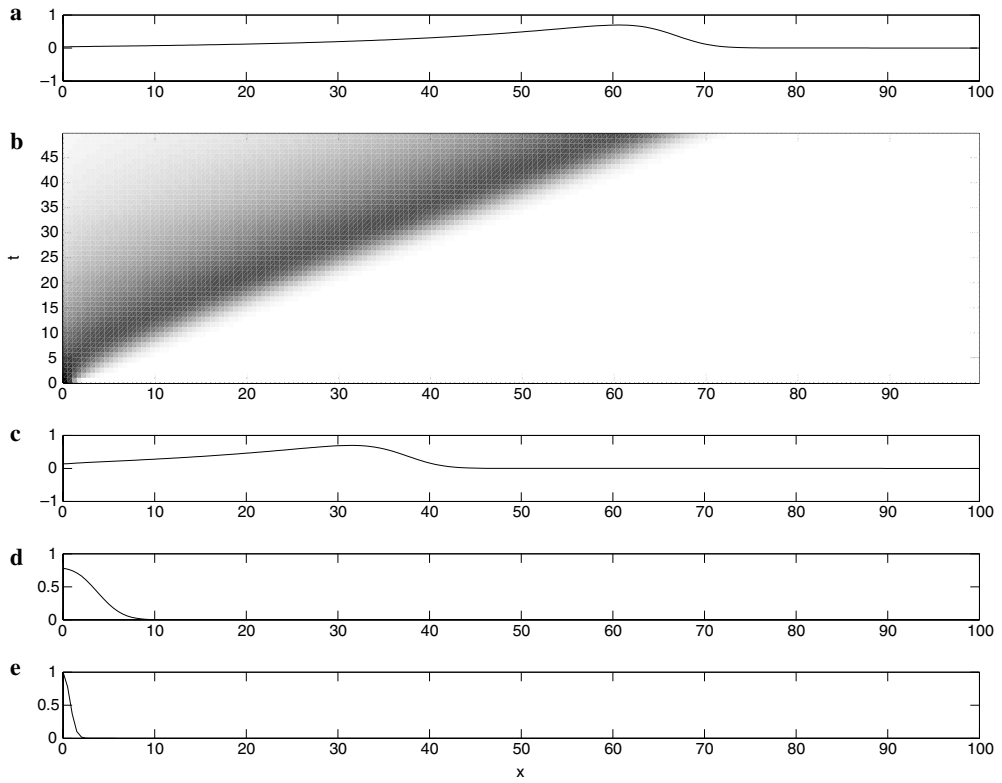

Fig. 3. Spreading of the infection wave. The density of infected as a function of coordinate is shown in panel (b) on a greyscale. Panels (e), (d), (c), and (a) show the forms of infection wave at times $t = 0$, 5, 30, and 50 days, respectively, as following from the solution of Eq. (7) with parameters listed in the text.

$\lambda = -0.95$, due to the fact that the one was still not in an asymptotic range for the size of the system and for the simulation time corresponding to realistic values of parameters adopted in computation. This shows that the form of the front relaxes to its asymptotic behavior considerably slower than its velocity does.

Let us now consider a change of the shape of disease wave under variation of susceptibility and a recovery rates, now irrespectively to experimental data. Fig. 5 represents a shape of the wave (left) the forward and the rear fronts in logarithmic scale (right) for different values of parameters chosen in such a way that the velocity of the wave stays constant (the same as in our previous calculation), however, the distance form criticality in these three waves is different, since the product $\kappa\tau$ assumes different values. The solid line corresponds to the parameters used above with $\kappa = 0.75$ and $\tau = 15$, the dashed and dotted lines are the solutions with $\kappa = 0.8$, $\tau = 6.25$, and $\kappa = 1$, $\tau = 2.0$, respectively. In all these cases both forward and rear fronts of the wave show clear exponential behavior, as seen in the left panel. The exponential decrement of the forward front exhibits a rather small change, due to the fact that for a fixed velocity it is given by $\lambda \approx v/2\tilde{D} = va^2/\kappa$, and the changes in κ are small. The numerical / theoretical values of the decrements at $t = 50$ for the last two cases are $-0.74/-0.89$ and $-0.61/-0.71$. On the contrary, the

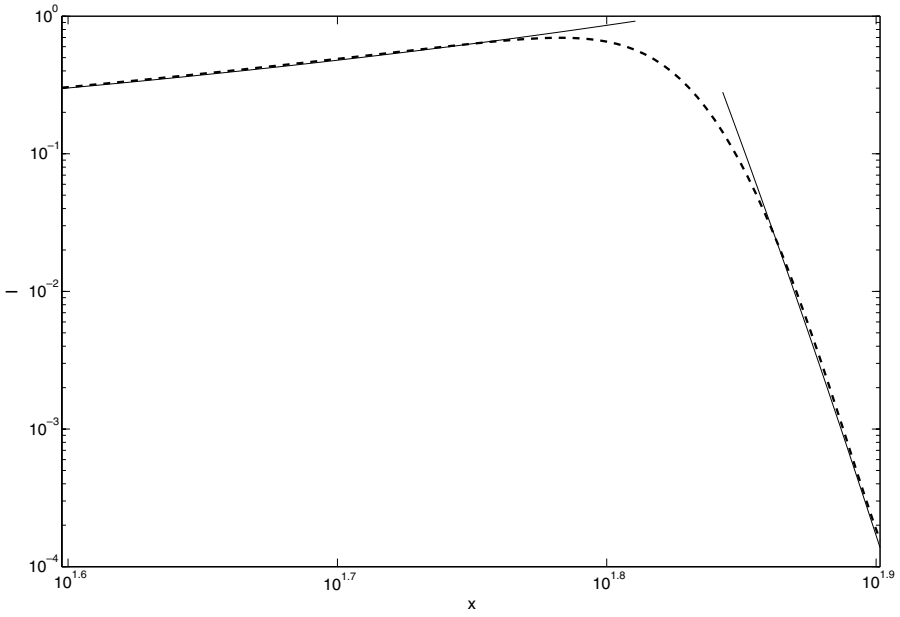

Fig. 4. Infection wave on a logarithmic scale.

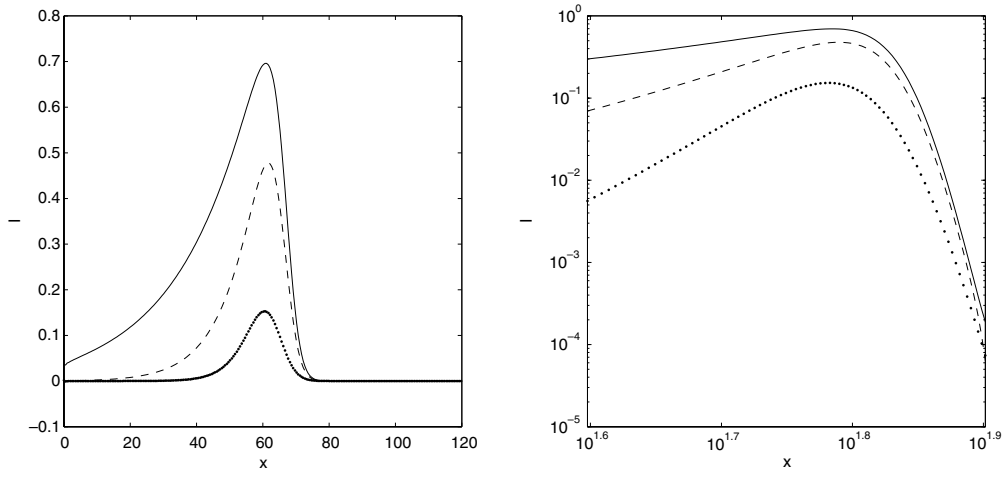

Fig. 5. Infection front form at the same time ($t = 50$) for the waves with the same velocity but with different value of the parameter $\kappa\tau$, see text for details.

changes in the tail slope are considerable: The measured/theoretical values of increments of the exponential growth here are: 0.11/0.11 and 0.25/0.35. This verifies the observation of strongly asymmetric Kendall waves in the strongly supercritical case which turn less asymmetric if the situation gets closer to criticality.

5. Summary

We considered infection spreading in a contact mode of disease propagation in an population whose members are immobile or strongly confined in their motion. We derive the corresponding mean field equation and show that its solution gives propagating infection waves of asymmetric shapes, resembling Kendall waves observed in real infections. We moreover present the results of numerical solution of our equations for realistic values of parameters obtained from field epidemiological data for a phocine distemper virus infection among harbor seals in 1988.

Acknowledgment

E.B. Postnikov is thankful to DAAD for financial support during his stay at the Humboldt University.

References

[1] C.A. Gilligan, Modelling soil-born pathogens: reaction–diffusion models, Can. J. Plant Pathol. 17 (1995) 96.
[2] J.D. Murray, Mathematical Biology II, Springer, 2003.
[3] W.O. Kermack, A.G. McKendrick, A contribution to the mathematical theory of epidemics, Proc. R. Soc. Lond. A 2003 V. 115, P. 700–721 1927.
[4] Thus, Murray, Ref. [2], does not interpret the corresponding diffusion coefficient as a diffusion coefficient of physical persons, but estimates it from the velocity of information (news) spread. This observation is indeed very old: already in the 18th century is was noted that, for example, the influenza epidemics of 1782 spread at the velocity of mail, see e.g., S. Winkle, *Kulturgeschichte der Seuchen*, Komet, Frechen, 1997, p. 1035 ff.
[5] A. Cliff, P. Haggett, Atlas of disease distributions: analytic approaches to epidemiological data, Blackwell, 1993.
[6] W. Otten, J.A.N. Filipe, C.A. Gilligan, An empirical method to estimate the effect of soil on the rate for transmission of damping-off disease, New Phytologist. 162 (2004) 231.
[7] L.M. Sander, C.P. Warren, I.M. Sokolov, Epidemics, disorder, and percolation, Physica A 325 (2003) 1.
[8] J. Swinton, J. Harwood, B.T. Grenfell, C.A. Gilligan, Persistence threshold for phocine distemper virus infection in harbour seal Phoca vitulina metapopulations, J. Anim. Ecol. 67 (1998) 54.
[9] A.J. Aceves, T. Dohnal, I. Gabitov, J.M. Hyman, Continuum Models of Disease Spreading – one and two species model, (unpublished, http://www.math.ethz.ch/dohnal/).
[10] L.F. Lopez, F.A.V. Coutinho, M.N. Burattini, E. Massad, Modelling the spread of infections when the contact rate among individuals is short ranged: Propagation of epidemic waves, Math. Comput. Model. 29 (1999) 55.
[11] M.N. Kuperman, H.S. Wio, Front propagation in epidemiological models with spatial dependence, Physica A 272 (1999) 206.
[12] L.M. Sander, G.V. Ghaisas, Fractals and patters in catalysis, Physica A 233 (1996) 629.
[13] R. Ball, M. Nauenberg, T.A. Witten, Diffusion-controlled aggregation in the continuum approximation, Phys. Rev. A 29 (1984) 2017.
[14] A.B. Ryabov, E.B. Postnikov, A.Yu. Loskutov, Diffusion-limited aggregation: a continuum mean field model, JETP 101 (2005) 253.
[15] P. Grassberger, On the critical behavior of the general epidemic process and dynamic percolation, Math. Biosci. 63 (1983) 157.
[16] L.M. Sander, C.P. Warren, I.M. Sokolov, C. Simon, J. Koopman, Percolation on disordered networks as a model for epidemics, Math. Biosci. 180 (2002) 293.
[17] R. Dietz, M.-P. Heide-Jørgenson, T. Harkønen, Mass death of harbour seals Phoca vitulina in Europe, Ambio 18 (1989) 258.